

Origin of the n -type and p -type conductivity of MoS₂ monolayers on a SiO₂ substrate

Kapildeb Dolui, Ivan Rungger and Stefano Sanvito
School of Physics and CRANN, Trinity College, Dublin 2, Ireland
 (Dated: January 14, 2013)

Ab-initio density functional theory calculations are performed to study the electronic properties of a MoS₂ monolayer deposited over a SiO₂ substrate in the presence of interface impurities and defects. When MoS₂ is placed on a defect-free substrate the oxide plays an insignificant role, since the conduction band top and the valence band minimum of MoS₂ are located approximately in the middle of the SiO₂ band-gap. However, if Na impurities and O dangling bonds are introduced at the SiO₂ surface, these lead to localized states, which modulate the conductivity of the MoS₂ monolayer from n - to p -type. Our results show that the conductive properties of MoS₂ deposited on SiO₂ are mainly determined by the detailed structure of the MoS₂/SiO₂ interface, and suggest that doping the substrate can represent a viable strategy for engineering MoS₂-based devices.

PACS numbers:

I. INTRODUCTION

Recently MoS₂-based layered transition metal chalcogenides (LTMDs) have attracted considerable attention due to their potential for constructing low dimensional nano-structures for a variety of applications¹⁻³. The electronic properties of MoS₂ show a strong dependence on thickness⁴, i.e. on the number of atomic layers forming a given sample. In particular, MoS₂ monolayers, which display a substantial direct band-gap, represent a semi-conducting alternative to graphene, which is a metal in its pristine form. Although the band-gap of graphene can be opened by fabricating nanoribbons⁵ or by depositing it on a suitable substrate⁶, this comes at the prize of deteriorating, in a somehow uncontrollable way, the carrier mobility due to edges and impurity scattering⁷. In contrast, the low dimensionality, the small amount of dangling bonds, and their typical high crystalline form, make the performances of LTMD-based transistors comparable to those of existing Si-based ones⁸⁻¹⁰. In particular transistors made from MoS₂ monolayers have been recently fabricated, showing a mobility of at least 200 cm²/V·s at room temperature, an on/off current ratio of 10⁸ and low standby power dissipation¹¹.

Interestingly, both n -type¹¹⁻¹⁴ and p -type^{15,16} conductivities have been reported in ultra-thin MoS₂ layers deposited on SiO₂. The conducting behavior of MoS₂ therefore seems to depend on the experimental details and an explanation for the specific current polarity (n - or p -type) remains far from being clear. Note that no intentional doping was introduced in the experiments mentioned above, so that the source of the different carrier types should be intrinsic to the MoS₂ layer, to the substrate and to the interaction between the two.

The possible creation of Mo and/or S vacancies during the growth cannot be the cause of the various conductive properties, since vacancies create deep levels at mid-gap in the bandstructure of MoS₂ monolayers¹⁷. Notably, disorder at the semiconductor/substrate interface in general plays a crucial role in determining the conductive properties of ultra-thin devices. For example,

for GaAs nanowires it has been demonstrated that upon decreasing the nanowire diameter the interface-mediated conductivity gradually becomes dominant over the bulk one¹⁸. Such surface sensitivity can also be used to one's advantage. For instance an ambipolar transistor has been realized in MoS₂ thin flakes by contact with an ionic liquid environment¹⁹, which as well affects the interface properties. Since MoS₂ monolayers are placed on insulators in practically any device architecture, it is important to identify the possible effects that the substrate has on the conductivity.

The defects responsible for the conductive properties of low dimensional devices are expected to be extrinsic in nature, such as charged impurities at the interface between the conductive channel and the substrate. These lead to an inhomogeneous Coulomb potential for both conduction and valence band electrons. Such charge traps have been identified to be in the form of adsorbates or defects at the surface of the underlying substrate in the case of graphene^{20,21}. Likewise, temperature dependent transport measurements on thin MoS₂ layers, down to the monolayer limit, suggest that trapped charges at the SiO₂ surface could be responsible for the observed n -type behavior, when MoS₂ is deposited on SiO₂²².

In general when charged traps are located at an interface, they influence the depletion/accumulation of electrons in the conducting channel up to a certain thickness, which is proportional to the channel screening length. This distance depends on different physical features, such as the nature and the density of the traps, and the electronic properties of the channel. For conventional semiconductors it typically reaches up to a few nanometers. For instance it has been recently demonstrated that charged trap states at the substrate/channel interface significantly affect the conductivity of GaAs nanowires up to diameters of about 40-70 nm¹⁸. More dramatic effects are expected for layered compounds down to the single layer limit, in which essentially all the atoms are at the interface with the substrate and the channel vertical dimension is certainly shorter than the screening length. Recently a reduction in conductivity with increasing the

MoS₂ film thickness has been observed in MoS₂-based transistors, where SiO₂ was used as back gate²³. This suggests that for the MoS₂/SiO₂ system the transport is interface-mediated, as intrinsic defects, homogeneously distributed in MoS₂, would not lead to any dependence of the conductivity on thickness.

In order to shed some light on the effects that trap states at the SiO₂ surface have on the conductive properties of MoS₂/SiO₂ hybrid systems, we have performed state of the art first principle electronic structure calculations. In particular we have considered the case when the traps are due to impurities such as immobile Na and H atoms, and O-dangling bonds. The paper is organized as follows. In the next section we briefly describe our computational techniques and we provide details of the simulations performed. Then we proceed with presenting the results of this work in the context of recent experiments, and finally we conclude.

II. METHODOLOGY

In order to investigate the influence of a SiO₂ substrate on the electronic properties of a MoS₂ monolayer, *ab-initio* calculations are performed by using density functional theory (DFT)^{24,25} within the generalized gradient approximation (GGA) of the exchange and correlation (XC) functional as introduced by Perdew, Burke and Ernzerhof (PBE)²⁶ and numerically implemented in the SIESTA code²⁷. In our calculations, a double- ζ polarized²⁸ numerical atomic orbital basis set is used for all the atoms and the Troullier-Martins scheme is employed for constructing norm-conserving pseudopotentials²⁹. An equivalent plane wave cutoff of 350 Ry is chosen in all the simulations and the Brillouin zone is sampled by using an equivalent k -grid cutoff of 17 Å. Relaxed geometries are obtained with the conjugate gradient method, where all the atoms in the supercell are allowed to relax until the force on each atom is less than 0.02 eV/Å.

A trap state is usually formed when an energy level associated either to a defect or an impurity appears within the energy gap of the host material. Such trap states influence the charge transport properties mainly in two ways. Firstly, if the traps are charged, they will capture a hole or an electron from the environment. This produces a modification of the electrostatic potential, which in turns shifts the level alignments in the system, and thus affects the conductivity. Secondly, they can also increase the carrier concentration and provide pathways for electrons or holes to hop. The efficiency of this process depends on the amount of localization of the states associated to the defect site. If the energy of the localized gap state is close to either the valence band maximum (VBM) or the conduction band minimum (CBM), then at a given temperature some of these charges will be transferred either to the conduction or to the valence band, where they may contribute to increase the system conductivity.

Whether or not one can describe with *ab initio* calcu-

lations such mechanisms depends crucially on the ability of computing accurately the energy levels of the system. The use of the GGA (or of the local density approximation - LDA) for electronic structure calculations of defect levels is, in general, problematic. One reason is the typical underestimation of the energy gap and the related incorrect alignment of the energy levels of hybrid systems. For instance an artificially reduced band-gap may erroneously bring deep traps in resonance with either the conduction or the valence band^{30,31}. A second source of error is the incorrect description of the charge localization at the defect site, a feature that usually leads to predict defects to be too shallow³². Atomic self-interaction correction (ASIC)^{33,34} has been proved to overcome these deficiencies^{35,36}. Therefore we also perform additional LDA+ASIC calculations to verify the robustness of the LDA/GGA results. In particular we set the ASIC scaling parameter to $\alpha = 0.5$, a value which is generally appropriate to mid-gap insulators³³.

III. RESULTS AND DISCUSSION

A. Defect-free SiO₂ interface

Substantial experimental efforts have been devoted to deposit ultra-thin MoS₂ layers onto SiO₂ in order to demonstrate transistor operation, down to the single layer limit^{11,12,16}. Usually amorphous oxides are used as substrates. However, in order to avoid the computational complexity of a highly disordered structure, a crystalline SiO₂ substrate is simulated here instead. This also allows us to systematically determine the effects of individual defects and impurities on the electronic structure of a MoS₂ layer. Our unit cell is constructed as a slab containing at least 6 Si atomic layers of α -quartz and an adsorbed MoS₂ monolayer. At least 15 Å of vacuum are included at the slab boundaries to avoid the spurious interaction between the slab periodic images. We consider the modified oxygen-terminated (0001) SiO₂ surface in order to simulate the most experimentally relevant conditions.

Two primary structures for the oxygen-terminated SiO₂ (0001) surface are possible, depending on whether the termination is with the siloxane group (Si-O-Si) or with the silanol one (Si-OH). Both surfaces can form depending on the surface treatment³⁷. The siloxane reconstruction at room temperature forms an O-terminated surface with an outermost six-membered ring structure, as shown in Fig. 1(a, b). Under annealing in ambient conditions it becomes hydroxylated (Si-OH) and the reconstruction transforms into the silanol one, which presents on the surface a zigzag H-bonded network [see Fig. 1(c, d)]. In both cases in our simulations the dangling bonds on the Si-terminated bottom surface are saturated by hydrogen.

The optimized lattice constants of the pristine SiO₂ and MoS₂ are 4.91 Å and 3.19 Å, respectively. We there-

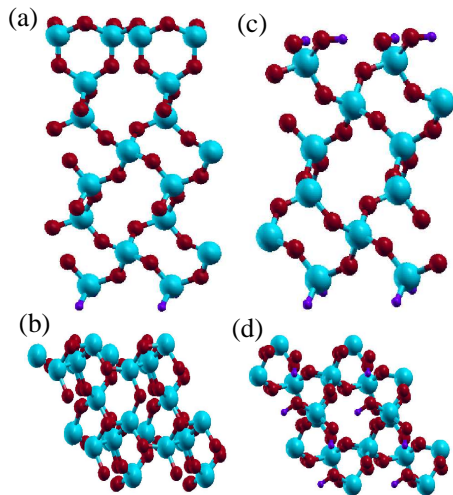


FIG. 1: (Color online) Side and top views of reconstructed structures for the O-terminated SiO₂ (0001) surface (a and b), and the fully hydroxylated SiO₂ (0001) one (c and d) (color code: cyan → Si, red → O, violet → H).

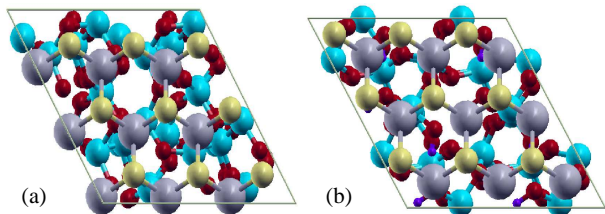


FIG. 2: (Color online) Top view of the optimized structure of MoS₂ placed on a defect-free (a) siloxane and (b) silanol surface (color code: light grey → Mo, yellow → S, cyan → Si, red → O, violet → H).

fore construct a hexagonal supercell in the plane, with a 9.69 Å-long side, so that the lattice mismatch between SiO₂ and MoS₂ is minimized to $\sim 1.2\%$. The GGA calculated band-gap of SiO₂ and of a MoS₂ monolayer are 6.20 eV and 1.49 eV, respectively. The small strain applied to the MoS₂ monolayer changes only little the electronic structure. The band-gap remains direct at the K point and it is only reduced by 0.22 eV from the value of 1.71 eV obtained for the unstrained case. Similarly to the case of graphene³⁸, we expect that the electronic structure of a MoS₂ monolayer is only marginally affected by its local arrangement on the SiO₂ substrate. Therefore, as a representative configuration we use the arrangement of Fig. 2, where an oxygen atom is situated at the hollow site of the Mo surface triangles.

We start our discussion by presenting the properties of the defect-free hybrid MoS₂/SiO₂ system. The equilibrium distances, d_0 , between the SiO₂ and the MoS₂ surfaces are 3.01 Å and 2.98 Å for siloxane and silanol, respectively. Here d_0 is defined as the vertical separation between the top-most O layer in the SiO₂ surface and its nearest S layer in MoS₂. These values are sim-

ilar to the distance between two MoS₂ monolayers that we calculate to be 3.17 Å. The binding energy of the MoS₂/SiO₂ system is given by $E_b = E_{\text{MoS}_2} + E_{\text{SiO}_2} - E_{\text{MoS}_2/\text{SiO}_2}$, where E_{MoS_2} , E_{SiO_2} , and $E_{\text{MoS}_2/\text{SiO}_2}$ are total energies of the isolated MoS₂, the isolated SiO₂ slab, and of the MoS₂/SiO₂ hybrid system, respectively. We find E_b for siloxane and silanol to be respectively 0.14 eV and 0.16 eV per primitive MoS₂ unit cell. These binding energies are close to that between two MoS₂ layers (0.20 eV/unit cell), which are bound together by the rather weak van der Waals forces. As such, our results show that MoS₂ is weakly bound also to the SiO₂ surface, in agreement with recent experimental results that have measured the interaction between MoS₂ and an underlying SiO₂ substrate to be negligible³⁹.

Note that in general GGA-type XC-functionals do not describe accurately van der Waals forces. However, it has been shown that the LDA/GGA is able to reproduce the interlayer spacing and the binding energy of layered chalcogenides⁴⁰. We have then verified that our calculated d_0 for bulk MoS₂, $d_0 = 3.08$ Å, is in good agreement with the experimental value of 2.96 Å⁴¹ and also with the previously calculated theoretical estimate of 3.05 Å⁴². Moreover, in order to take into account possible small deviations of the relaxed distance from the experimental value due to the XC functional used, we have evaluated the electronic structure for d_0 within the range $d_0 \pm 0.5$ Å, and we have found that the results change little with varying the distance.

B. SiO₂/MoS₂ composite with siloxane reconstruction

We now move to study the electronic structure of a MoS₂ monolayer deposited on SiO₂ by starting with the siloxane surface. In particular we consider first the situation where SiO₂ is defect-free. Fig. 3(c) shows the density of states (DOS) of the hybrid SiO₂/MoS₂ system, which remains semiconducting with a band-gap of 1.48 eV, i.e. with the same band-gap of a free-standing MoS₂ monolayer having the same lattice parameters. Both the valence and the conduction bands of the hybrid compound are associated to MoS₂. We note that the projected DOS (PDOS) over MoS₂ extends into the SiO₂ band-gap, and the total DOS of the combined material is essentially given by the superposition of the DOSs of the pristine slab of SiO₂ [Fig. 3(a)] and of the MoS₂ monolayer [Fig. 3(b)]. Both the conduction and the valence bands of SiO₂ are located at least 1.5 eV away from those of MoS₂. As a consequence, no charge transfer between the substrate and MoS₂ occurs. Importantly, one of the basic criteria for the selection of the gate oxide is fulfilled here, namely that the oxide should have a bands offset of over 1 eV for both the conduction and valence band in order to create a large barrier for both electrons and holes⁴³. Our results show that the conductivity of MoS₂ is not influenced by the underlying defect-free SiO₂ sub-

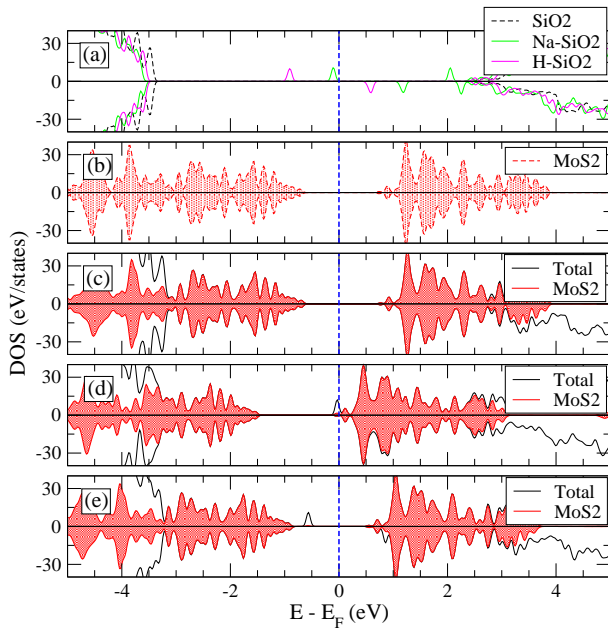


FIG. 3: (Color online) Electronic structure of the $\text{SiO}_2/\text{MoS}_2$ hybrid system when various defects are present at the SiO_2 siloxane surface. (a) The total DOS for the defect-free surface (black, dashed curves), and when either Na (green, solid curves), or H adsorbed (magenta, solid curves) are adsorbed. (b) The DOS of a pristine free-standing MoS_2 monolayer. The total DOS and the PDOS for MoS_2 , when the MoS_2 monolayer is placed on the defect-free siloxane surface (c), on a siloxane surface with one adsorbed Na, or (d) with one adsorbed H. The blue dashed vertical line indicates the Fermi level, which has been set to zero in all the panels. The red shaded areas indicate the MoS_2 PDOS. Positive and negative DOS are respectively for spin up (majority spins) and spin down (minority spins) electrons.

strate. Therefore the measured n -type or p -type conducting properties of MoS_2 on SiO_2 must be due to defects and impurities.

Localized states, arising from impurities or defects within the oxide substrate or at the interface with the conducting channel, can redefine the effective Fermi level of the hybrid system, as illustrated schematically in Fig. 4. Depending on the alignment of the gap states with respect to the MoS_2 valence and conduction bands, the system can switch from n -type [see Fig. 4(b)] to p -type [see Fig. 4(c)]. Therefore, such trap states are expected to give significant contributions to the conductivity of these low dimensional systems. In the layered structure considered in this work, the trap states are expected to be located at the interface between the LTMDs and the substrate, not in the LTMDs themselves, which usually are highly defect-free. Trap states at the SiO_2 surface can have a wide range of origins, such as immobile ionic charges, SiO_2 surface dangling bonds, and foreign impurities adsorbed on the surface⁴⁴. In literature densities of trap states on SiO_2 are reported in the range⁴⁵ 10^{10} - 10^{14} cm^{-2} . As representative dopants, here we consider two

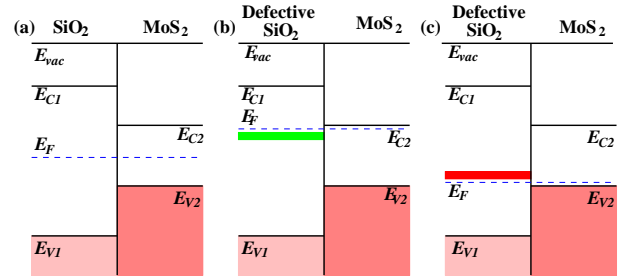


FIG. 4: (Color online) Schematic band diagram for MoS_2 placed on the defect SiO_2 substrate (a), and on a substrate including a defect-induced donor (b) or acceptor (c) level. This demonstrates the modulation of the conductivity from n -type to p -type as the impurity state redefines the Fermi energy in the oxide. The energy levels E_V , E_C , E_F and E_{vac} define the valence band maximum (VBM), the conduction band minimum (CBM), the Fermi energy, and the vacuum level, respectively. The subscripts 1 and 2 refer to SiO_2 and MoS_2 , respectively. The blue dashed-lines indicate the Fermi energy of the hybrid system (common to SiO_2 and MoS_2). The thick green line in (b) indicates the donor level and the thick red line in (c) represents the acceptor state in the oxide. Note that in general due to charge transfer from MoS_2 to the gap states, and the related dipole formation, the level alignment between E_{V1} and E_{V2} will also change in the defective systems.

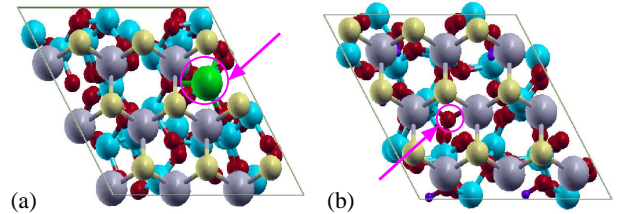


FIG. 5: (Color online) The optimized geometry for MoS_2 placed on (a) the siloxane surface incorporating a Na impurity and (b) the dangling oxygen bond on the silanol surface, obtained by removing a H atom. The arrows indicate the positions of the defects on the surface (Color code: green \rightarrow Na, while the other colors are the same atoms as in Fig. 2). The arrows indicate the location of the impurities/defects.

possible candidates: Na atoms and SiO_2 surface oxygen dangling bonds.

During the synthesis and the sample preparation, SiO_2 can adsorb relatively light impurities such as Na and K ⁴⁶ at its surface. In order to simulate the effects of such impurities on the electronic structure of the MoS_2 channel a single Na atom is placed on top of the siloxane SiO_2 surface. Given the lateral dimension of our supercell, this corresponds to an impurity density of $\sim 10^{14}$ cm^{-2} , which is close enough to the recently reported values of trap states densities, reaching up to $\sim 10^{13}$ cm^{-2} for thin MoS_2 layers deposited on SiO_2 ^{8,23}. The most energetically favorable binding position for Na is found to be at the center of the surface oxygen triangle [see panel (a) of Fig. 5]. A Na adatom adsorbed on a pristine SiO_2 sur-

face creates a deep donor state in the DOS, with a single particle level at about 2 eV below the SiO₂ CBM [see Fig. 3(a)]. Note that such state is singly occupied and therefore spin-splits in our spin-polarized calculations, with the empty minority spin state (spin down) laying approximately 1 eV below the CBM and 1 eV below the Fermi level.

When a MoS₂ monolayer is deposited over the the Na-doped SiO₂ surface, d_0 increases to 3.24 Å at the edges of our unit cell, whereas at the Na site the O-S distance becomes 3.45 Å. The enlargement of the binding distance compared to that of the pristine SiO₂/MoS₂ system is a direct consequence of the Na intercalation at the interface. The electronic structure of the composite is strongly affected by the presence of the Na ion, as shown in Fig. 3(c). Also in this case the total DOS appears as a direct superposition of those of SiO₂ and MoS₂. However the presence of the Na filled state shifts the Fermi level, which now gets pinned just below the MoS₂ CBM. The resulting DOS around E_F is thus that of the defect-free MoS₂ conduction band with the addition of a Na-derived impurity level positioned below it. Hence, the gap state is moved below the Fermi energy, resulting in a very small activation energy for the transfer of electrons from Na to the MoS₂ conduction band. This is the situation schematically presented in figure 4(b), which leads to n -doping.

If we now replace Na with H on the SiO₂ siloxane surface, the associated filled gap state lies deep in the SiO₂ band-gap [see Fig. 3(a)], despite the fact that H and Na share the same s -like valence. The same situation persists in the composite [see Fig. 3(e)], where the H-derived filled spin-up level remains at mid-gap, approximately 0.5 eV above the VBM, while the empty spin-down one is nearly resonant within the conduction band. This situation however does now lead to doping so that H can not influence the conductivity of the MoS₂/SiO₂ structure. The quantitative difference found between the results for the Na and the H case show that, in order to obtain n -type character, only impurities with rather small ionization potential are relevant. These can transfer one electron to the MoS₂ conduction band with small activation energy. Such activation energy is a key factor in the determination of the threshold voltage, V_{th} , required to operate a transistor in the on-state. As a consequence, the experimentally measured values for V_{th} , which show a large variation for different samples²², are then attributable to varying concentrations and properties of the trap states from sample to sample.

C. SiO₂/MoS₂ composite with silanol reconstruction

Next we move to examine the case of the SiO₂ surface with silanol reconstruction, whose DOS is presented in Fig. 6(a). Similarly to the siloxane case, the PDOS for the defect-free MoS₂/SiO₂ composite [see Fig. 1(b)]

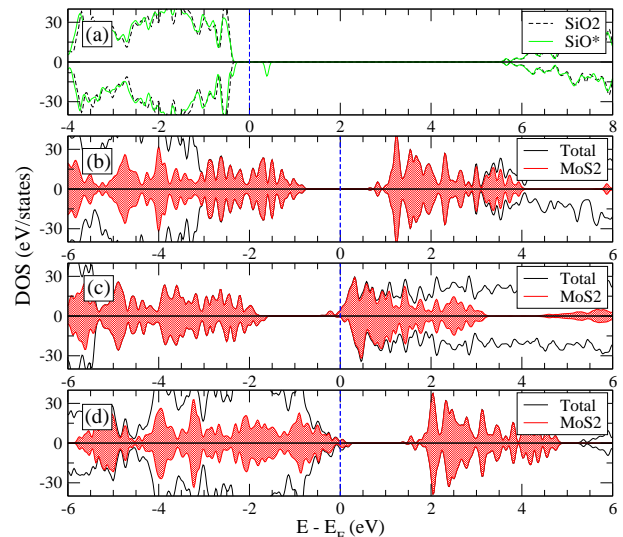


FIG. 6: (Color online) Electronic structure of the SiO₂/MoS₂ hybrid system when various defects are present at the SiO₂ silanol-reconstructed surface. (a) The DOS for the defect-free surface (black, dashed curve) and for the one where one O dangling bond is induced by a single H removal (green, solid curve labelled as SiO*). The total DOS and the MoS₂ PDOS for the SiO₂/MoS₂ composite when the MoS₂ monolayer is placed on (b) the defect-free surface, (c) on the surface with a single adsorbed Na atom, and (d) on the surface with a O dangling bond created by removing a single H atom. The blue dashed line indicates the Fermi energy, which is set to zero in all panels. The red shaded areas indicate the MoS₂ PDOS. Positive and negative DOS are respectively for spin up (majority spins) and spin down (minority spins) electrons.

corresponds to a superposition of the DOSs of the isolated MoS₂ [Fig. 3(b)] and SiO₂ [Fig. 6(a)] components, indicating weak interaction between the two materials. When a Na atom is intercalated between the silanol surface and the MoS₂ layer, we find that the system becomes n -type [Fig. 6(c)], in the same way as for the siloxane surface. This indicates that Na is an efficient n -dopant for MoS₂ on SiO₂ regardless of the surface reconstruction.

In general thermal annealing of the silanol surface creates under-coordinated oxygen atoms (Si-O*). These appear as stable surface defect centers and act as typical charge traps in oxygen rich SiO₂⁴⁷, since they are able to capture an extra electron in their dangling bond. In our calculations, such defects are created on the Si-OH surface by removing a H atom from the top surface [see Fig. 5(b)]. For such a defect we find that the empty acceptor state is created ~ 0.9 eV above the SiO₂ VBM [see Fig. 6(a)]. Once MoS₂ is layered onto the surface, the value of d_0 at the boundary of our H-deficient unit cell is $d_0 = 2.98$ Å, which is approximately equal to that for the pristine surface, whereas at the dangling bond site the O-S distance is significantly reduced to 2.68 Å. When placing the MoS₂ monolayer on this defective surface, the dangling bond state gets filled by capturing an electron from the MoS₂ valence band, so that the Fermi

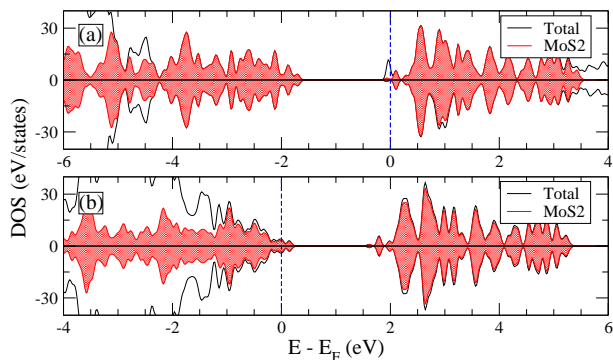


FIG. 7: (Color online) Density of states for the defective $\text{SiO}_2/\text{MoS}_2$ composite calculated with the ASIC XC functional. In panel (a) we report the DOS for the siloxane reconstruction with an intercalated Na atom [corresponding to Fig 3(d)], while in (b) that for the silanol reconstruction and an O dangling bond obtained by removing a surface H atom [corresponding to 6(d)].

energy now lies just below the MoS_2 VBM [see Fig. 6(d)]. This is the level alignment presented in Fig. 4(c), which makes the composite p -type. Note that the rather high density of oxygen dangling bonds in our system causes a large surface charge density dipole, which shifts the MoS_2 DOS downwards in energy by more than 1 eV with respect to the SiO_2 substrate. By modulating the density of such defect types one may be able to change such a shift.

D. Robustness of the results against the choice of XC functional: ASIC

Finally, in order to verify that the calculated level alignment is robust against the choice of exchange and correlation functional, we have repeated our calculations by using the ASIC scheme. As expected the ASIC functional increases the band-gap of MoS_2 and SiO_2 respectively to 1.73 eV and 8.02 eV (for the same strained hybrid structure used in the previous sections). In the case of SiO_2 this brings the calculated value sensibly closer to the experimental one of 8.9 eV⁴⁸, as expected from the ASIC when dealing with an insulator whose valence and conduction bands have different orbital content^{33,34}.

The situation for MoS_2 is more complicated and deserves a detailed discussion. In this case the band-gap is defined by bands dominated mainly by Mo- d orbitals and the ASIC opens it only marginally. For a free-standing MoS_2 monolayer the ASIC ($\alpha = 0.5$) returns a direct band-gap of 2.03 eV (compared to a GGA gap of 1.71 eV). Note that the LDA value is 1.87 eV so that the LDA already partially opens the gap with respect to the GGA. It is also notable that an enhancement of the screening parameter α to $\alpha = 1$ (full atomic correction) produces a marginal further increase of the gap to 2.10 eV. Im-

portantly the ASIC result is rather close to that calculated⁴⁹ with the hybrid Heyd-Scuseria-Ernzerhof (HSE) exchange-correlation functional⁵⁰. This is however larger than the optical band-gap of 1.90 eV measured experimentally for MoS_2 monolayers¹². The apparent contradiction can be solved by noting that the optical excitations involve excitons with a large binding energy of the order of 1 eV, as confirmed by many-body calculations⁴⁹. Thus, one expects that the true quasi-particle spectrum has a band-gap of approximately $1.9+1=2.9$ eV, in good agreement with that computed with the GW scheme, either at the first order level⁴⁹ (2.82 eV) or self-consistently⁵¹ (2.76 eV). As such, the ASIC describes MoS_2 with a band-gap larger than the measured optical one and it provides an improved description over that of the GGA.

We now go back to the $\text{SiO}_2/\text{MoS}_2$ composite and in Fig. 7 we report two representative results for the case of Na adsorbed on the siloxane surface and for that of the O dangling bond on the silanol one. We find that for the first case, although the band-gaps of the two parental materials are both increased, the Fermi energy is still pinned at the bottom of the MoS_2 conduction band [Fig. 7(a)]. As a consequence Na still leads to a n -type semiconducting character with small activation barrier. Similarly the O dangling bond on the silanol-terminated surface leads to a p -type semiconducting character [see Fig. 7(b)], with the Fermi energy positioned below the MoS_2 valence band. This indicates that our two main results remain unchanged whether calculated at the GGA or ASIC level, i.e. they are robust with respect to the choice of exchange-correlation functional.

IV. CONCLUSION

The effects of the SiO_2 substrate on the conductivity of a semiconducting MoS_2 monolayer are investigated with first principles density functional theory calculations. The defect-free SiO_2 surface does not affect significantly the electronic properties of MoS_2 due to their weak mutual interaction. As such the conductive properties of MoS_2 do not change and SiO_2 appear as an ideal gate material. However, when Na atoms are placed at the $\text{SiO}_2/\text{MoS}_2$ interface, a shallow donor trap state is created just below the CBM of the hybrid $\text{SiO}_2/\text{MoS}_2$ composite. The small activation energy makes the hybrid $\text{MoS}_2/\text{Na-SiO}_2$ system a n -type semiconductor even for rather low temperatures. Interestingly, the behavior is different for H adsorption, where the impurity level is created ~ 0.9 eV below the CBM, resulting in a stable localized charge that cannot be easily promoted to the CBM and does therefore not affect the conductivity.

In contrast, in the case of oxygen dangling bonds on the silanol-terminated SiO_2 surface, the Fermi energy of the $\text{MoS}_2/\text{SiO}_2$ system is located just below the VBM, making the system a p -type semiconductor. These results shows that the conductivity of ultra-thin semiconduct-

ing LTMDs changes from n -type to p -type depending on the charge-polarity of the traps, as well the energy level alignment of the trap states within the LTMDs band gap. These kind of trap states at the SiO₂ surface are likely to be at the origin of the observed change in conductance in different experimentally realized MoS₂-based transistors. Intriguingly, our results suggest the possibility of intentionally doping MoS₂ by depositing different adsorbates over the substrate SiO₂ surface. This can pave the way for a new strategy in the design of two-dimensional devices, where the electronic properties of the channel are engineered by manipulating those of the substrate.

Acknowledgments

This work is supported by Science Foundation of Ireland (Grant No. 07/IN.1/I945) and by CRANN. IR acknowledges financial support from the King Abdullah University of Science and Technology (ACRAB project). We thank Trinity Centre for High Performance Computing (TCHPC) for the computational resources provided.

- ¹ J. V. Lauritsen, J. Kibsgaard, S. Helveg, H. Topsøe, B. S. Clausen, E. Lægsgaard, and F. Besenbacher, *Nature Nanotech.* **2**, 53 (2007).
- ² Z. Yin, H. Li, H. Li, L. Jiang, Y. Shi, Y. Sun, G. Lu, Q. Zhang, X. Chen, and H. Zhang, *Acs Nano* **6**, 74 (2012).
- ³ Q.H. Wang, K. Kalantar-Zadeh, A. Kis, J.N. Coleman and M.S. Strano, *Nature Nanotech.* **7**, 699 (2012).
- ⁴ A. Splendiani, L. Sun, Y. Zhang, T. Li, J. Kim, C.-Y. Chim, G. Galli, and F. Wang, *Nano Lett.* **10**, 1271 (2010).
- ⁵ X. Wang, Y. Ouyang, X. Li, H. Wang, J. Guo, and H. Dai, *Phys. Rev. Lett.* **100**, 206803 (2008).
- ⁶ S. Y. Zhou, G.-H. Gweon, A. V. Fedorov, P. N. First, W. A. de Heer, D.-H. Lee, F. Guinea, A. H. Castro Neto and A. Lanzara, *Nature Materials* **6**, 770 (2007).
- ⁷ S. Adam, E. H. Hwang, V. M. Galitski, and S. D. Sarma, *PNAS* **104**, 18392 (2007).
- ⁸ A. Ayari, E. Cobas, O. Ogundadegbe, and M. S. Fuhrer, *J. Appl. Phys.* **101**, 014507 (2007).
- ⁹ K.-K. Liu, W. Zhang, Y.-H. Lee, Y.-C. Lin, M.-T. Chang, C.-Y. Su, C.-S. Chang, H. Li, Y. Shi, H. Zhang, C.-S. Lai, and L.-J. Li, *Nano Lett.* **12**, 1538 (2012).
- ¹⁰ L. Liu, S. B. Kumar, Y. Ouyang, and J. Guo, *IEEE Trans. Electron Devices* **58**, 3042 (2011).
- ¹¹ B. Radisavljevic, A. Radenovic, J. Brivio, V. Giacometti, and A. Kis, *Nature Nanotech.* **6**, 147 (2011).
- ¹² K. F. Mak, C. Lee, J. Hone, J. Shan, and T. F. Heinz, *Phys. Rev. Lett.* **105**, 136805 (2010).
- ¹³ H. Li, G. Lu, Z. Yin, Q. He, H. Li, Q. Zhang, H. Zhan, *Small* **8**, 682 (2012).
- ¹⁴ Y.-H. Lee, X.-Q. Zhang, W. Zhang, M.-T. Chang, C.-T. Lin, K.-D. Chang, Y.-C. Yu, J. T.-W. Wang, C.-S. Chang, L.-J. Li, and T.-W. Lin, *Adv. Mater.* **24**, 2320 (2012).
- ¹⁵ Z. Zeng, Z. Yin, X. Huang, H. Li, Q. He, G. Lu, F. Boey, and H. Zhang, *Angew. Chem. Int. Ed.* **50**, 11093 (2011).
- ¹⁶ Y. Zhan, Z. Liu, S. Najmaei, P. M. Ajayan, and J. Lou, *Small* **8**, 966 (2012).
- ¹⁷ C. Ataca, and S. Ciraci, *J. Phys. Chem. C* **115**, 13303 (2011).
- ¹⁸ N. Han, F. Wang, J. J. Hou, F. Xiu, S. Yip, A. T. Hui, T. Hung, and J. C. Ho, *ACS Nano* **6**, 4428 (2012).
- ¹⁹ Y. Zhang, J. Ye, Y. Matsushashi, and Y. Iwasa, *Nano Lett.* **12**, 1136 (2012).
- ²⁰ P. Joshi, H. E. Romero, A. T. Neal, V. K. Toutam, and S. A. Tadigadapa, *J. Phys.: Condens. Matter* **22**, 334214 (2010).
- ²¹ T. O. Wehling, A. I. Lichtenstein, and I. Katsnelson, *Appl. Phys. Lett.* **93**, 202110 (2008).
- ²² S. Ghatak, A. N. Pal, and A. Ghosh, *ACS Nano* **5**, 7707-7712 (2011).
- ²³ H. Liu, J. Gu, and P. D. Ye, *IEEE Electron Device Lett.* **33**, 1273 (2012).
- ²⁴ P. Hohenberg and W. Kohn, *Phys. Rev.* **136**, B864 (1964).
- ²⁵ W. Kohn and L. J. Sham, *Phys. Rev.* **140**, A1133 (1965).
- ²⁶ J. P. Perdew, K. Burke, and M. Ernzerhof, *Phys. Rev. Lett.* **77**, 3865 (1996).
- ²⁷ J. M. Soler, E. Artacho, J. D. Gale, A. Gracia, J. Junquera, P. Ordejón, and D. Sánchez-Porta, *J. Phys.: Condens. Matter* **14**, 2745 (2002).
- ²⁸ J. Junquera, Óscar Paz, D. Sánchez-Portal, and E. Artacho, *Phys. Rev. B* **64**, 235111 (2001).
- ²⁹ N. Troullier and J. L. Martins, *Phys. Rev. B* **43**, 1993 (1991).
- ³⁰ S. Sanvito and C.D. Pemmaraju, *Phys. Rev. Lett.* **102**, 159701 (2009).
- ³¹ A. Zunger, S. Lany and H. Raebiger, *Physics* **3**, 53 (2010).
- ³² A. Droghetti, C.D. Pemmaraju and S. Sanvito, *Phys. Rev. B* **78**, 140404(R) (2008).
- ³³ C.D. Pemmaraju, T. Archer, and D. Sánchez-Portal and S. Sanvito, *Phys. Rev. B* **75**, 045101 (2007).
- ³⁴ A. Filippetti, C.D. Pemmaraju, S. Sanvito, P. Delugas, D. Puggioni and V. Fiorentini, *Phys. Rev. B* **84**, 195127 (2011).
- ³⁵ A. Droghetti and S. Sanvito, *Appl. Phys. Lett.* **94**, 252505 (2009).
- ³⁶ C.D. Pemmaraju, R. Hanafin, T. Archer, H.B. Braun and S. Sanvito, *Phys. Rev. B* **78**, 054428 (2009).
- ³⁷ K. Nagashio, T. Yamashita, T. Nishimura, K. Kita, and A. Toriumi, *Journal of Appl. Phys.* **110**, 024513 (2011).
- ³⁸ N. T. Cuong, M. Otani, and S. Okada, *Phys. Rev. Lett.* **106**, 106801 (2011).
- ³⁹ S. W. Han, H. Kwon, S. K. Kim, S. Ryu, W. S. Yun, D. H. Kim, J. H. Hwang, J. S. Kang, J. Baik, H. J. Shin, and S. C. Hong, *Phys. Rev. B* **84**, 045409 (2011).
- ⁴⁰ T. Björkman, A. Gulans, A.V. Krasheninnikov and R. M. Nieminen, *Phys. Rev. Lett.* **108**, 235502 (2012).
- ⁴¹ J. A. Wollman and R. B. Somaono, *Phys. Rev. B* **13**, 3843 (1976).
- ⁴² C. Ataca, M. Topsakal, E. Akturk, and S. Ciraci, *J. Phys. Chem. C* **115**, 16354 (2011).
- ⁴³ J. Robertson and B. Falabretti, *J. Appl. Phys.* **100**, 014111 (2006).
- ⁴⁴ Narain Arora, *Mosfet Modeling For VLSI Simulation*,

- World Scientific Publishing Co. Pte. Ltd 2007, pp 128-129.
- ⁴⁵ R. A. McKee, F. J. Walker, and M. F. Chisholm, *Science* **293**, 468 (2001); Y.-W. Tan, Y. Zhang, K. Bolotin, Y. Zhao, S. Adam, E. H. Hwang, S. D. Sarma, H. L. Stormer and P. Kim, *Phys. Rev. Lett.* **99**, 246803 (2007); K. Nagashio, T. Yamashita, T. Nishimura, K. Kita, and A. Toriumi, *J. Appl. Phys.* **110**, 024513 (2011).
- ⁴⁶ Horacio E. Bergna, *The Colloid Chemistry of Silica*, *Advances in Chemistry*, Vol. 234 chapter 1, pp 1-47 (1994)
- ⁴⁷ M. Stapelbroek, D. L. Griscom, E. J. Friebele, and G.H. Sigel, *J. Non-Crystalline Solids* **32**, 313 (1979).
- ⁴⁸ B. El-Kareh, *Fundamentals of Semiconductor Processing Technologies*. Norwell: Kluwer Academic Publishers, 1995.
- ⁴⁹ A. Ramasubramaniam, *Phys. Rev. B* **86**, 115409 (2012).
- ⁵⁰ J. Heyd, G.E. Scuseria and M. Ernzerhof, *J. Chem. Phys.* **118**, 8207 (2003); J. Heyd, G.E. Scuseria and M. Ernzerhof, *J. Chem. Phys.* **124**, 219906 (2006).
- ⁵¹ T. Cheiwchanchamnangij and W.R.L. Lambrecht, *Phys. Rev. B* **85**, 205302 (2012).